Supplementary information

Carnosic acid biosynthesis elucidated by a Synthetic Biology platform

Codruta Ignea[a], Anastasia Athanasakoglou[a], Efstathia Ioannou[b], Panagiota Georgantea[b], Fotini A. Trikka[c], Sofia Loupassaki[d], Vassilios Roussis[b], Antonios M. Makris[c] and Sotirios C. Kampranis[a,1]

[a]*Department of Biochemistry, School of Medicine, University of Crete, P.O. Box 2208, Heraklion 71003, Greece*

[b]*Department of Pharmacognosy and Chemistry of Natural Products, School of Pharmacy, University of Athens, Panepistimiopolis Zografou, Athens 15771, Greece*

[c]*Institute of Applied Biosciences – Centre for Research and Technology Hellas (INAB-CERTH), P.O. Box 60361, Thermi 57001, Thessaloniki, Greece*

[d]*Mediterranean Agronomic Institute of Chania, P.O. Box 85, Chania 73100, Greece*

1. Supplementary Methods

1.1. Yeast media. Yeast cells were cultivated in Complete Minimal (CM) medium, composed of 0.13% (w/v) dropout powder (all essential amino acids), 0.67% (w/v) Yeast Nitrogen Base w/o AA (Y2025, US Biologicals) and 2% D-(+)-Glucose monohydrate (16301, Sigma). For galactose-based medium, glucose was substituted with 2% D-(+) Galactose (G0625, Sigma) and 1% Raffinose pentahydrate (R1030, US Biological).

1.2. Chemicals and enzymes.

Standard compounds geranyllinalool (Aldrich, 48809), geranylgeraniol (Sigma, G3278), sclareol (VIORYL SA. Athens, Greece), carnosic acid (Fluka, 91209) and carnosol (Cayman, 89800) were used. Other standards, such **6**, **7** and **15** were obtained from our in-house collection, isolated from natural sources and characterized by NMR analyses. **16**, **17** and **18** were produced and characterized in the context of this work. PCR amplifications were performed using Phusion High-Fidelity DNA Polymerase (New England BioLabs, M0530) and MyTaq DNA polymerase (BIO-21105, Bioline). For cloning purposes, restriction enzymes from New England BioLabs were used. NucleoSpin Plasmid Kit (740588, Macherey-Nagel) was used for plasmid DNA purification. QIAquick Gel Extraction Kit (#28704, Qiagen) was used for gel extraction and DNA purification.

1.3. Gene cloning and expression vectors

Constructs pYES2myc/ERG20-CcGGPPS, pWTDH3myc/SfCDS and pHTDH3myc/SpMilS are described in (1, 2).

The SfCDS ORF containing no stop codon and a 3xGS linker at the C-terminus was amplified using primers SfCDS-BamHI-5 and SfCDS-3xGS-MfeI (Table S5). The construct pYES/CcCLS-ERG20(F96C) previously described in ref. (2) was digested with *Bam*HI-*Eco*RI resulting in the removal of the CcCLS-5xGS fragment. The fusion SfCDS-ERG20(F96C) was generated by ligation of the SfCDS-3xGS fragment digested with *Bam*HI-*Mfe*I into *Bam*HI-*Eco*RI sites of pYES/ERG20(F96C).

High quality total RNA from *S. pomifera* trichomes or *R. officinalis* whole leaves was isolated using the commercial Spectrum Plant Total RNA Kit (Sigma Aldrich, St. Louis, MO, USA) according to the manufacturersô specifications. cDNA synthesis was carried out with reverse transcriptase SuperScript II-RT (Life Technologies, Carlsbad, CA, USA) following the manufacturerôs protocol. To generate constructs pESC-Leu::CPR2-SpCYP and pWTDH3myc/SpCYP, the open reading frames of *S. pomifera* CYPs were amplified with corresponding primers (Table S5) adding either an *Eco*RI or *Mfe*I site at the 5' end and a *Not*I site at 3' end and subcloned in pESC-Leu::CPR2 vector (3) and in pWTDH3myc vector (4), digested with *Eco*RI and *Not*I. To subclone *S. pomifera* CYPs under Leu selection, the vector pESC-Leu::CPR2 was modified to enable standardized CYPs cloning under the P_{GAL10} promoter into the *Eco*RI and *Not*I restriction sites. To this end, the *Eco*RI(1117) site from pESC-Leu backbone and the CPR2 internal *Eco*RI site were removed by double site-directed mutagenesis using primers pESC-noEcoRI and CPR2-noEcoRI (Table S5). Prior to generation of the

CYP716C12 and CYP71AU53 digested fragments, the corresponding pCRII-TOPO constructs were used as templates for site-directed mutagenesis for the removal of internal *Eco*RI or *Mfe*I sites using primers 5-U22595-noEcoRI or 5-U31529-noMfeI (Table S5), respectively.

Plasmid pENTR/SD/D-TOPO/CYP76AH4 was kindly provided by Prof. Reuben Peters (Iowa State University). The open reading frame of the *R. officinalis* ferruginol synthase, (CYP76AH4) was amplified to add *Eco*RI and *Not*I sites at 5' and 3' ends, respectively, using primers RoFS-EcoRI and RoFS-NotI (Table S5) and subcloned into the *Eco*RI and *Not*I sites of vector pESC-Leu::CPR2.

1.4. Yeast strain cultivation, terpene quantification, and extraction from yeast cells. Yeast cells were cultivated as previously described (1). Cultures grown until OD_{600} = 0.7-1 were switched to galactose-raffinose based selective growth medium (10 mL) for expression of the Erg20p-CcGGPPS and SpCDS-Erg20p(F96C) fusions, poplar CPR2 and CYP76AH24 or CYP76AH4 under the galactose-inducible promoters P_{GAL1} and P_{GAL10}. For production, cultures were cultivated for 2 days. Terpene extraction was performed by 10% dodecane overlay or solvent (pentane or ethyl acetate) extraction using aliquots of 1 mL cultures. Solvent extracts were derivatized prior to GC-MS analysis using the following procedure. After complete removal of the solvent, samples were treated with 100 εl of Sylon HTP (hexamethyldisilylazane:trimethylchlorosilane:pyridine, 3:1:9) (Supleco, Bellafonte, PA), mixed by vortexing and heated at 60 °C for 30 min. At the end of the incubation, the Sylon HTP solution was evaporated under a gentle stream of nitrogen, and samples were dissolved in 50 εL of n-hexane and mixed by vortexing. The compounds produced were quantified by GC-FID analysis of the solvent extracts, as described in (5), and identified by GC-MS based comparison with commercial or in-house standards.

It is formally possible that when two very closely related CYP genes are introduced as M3a and M3b parts in yeast, undesirable recombination events may be selected over time in the presence of selective pressure (e.g. formation of a toxic product). Although in our studies we did not obtain any indication that recombination occurs at a significant frequency, it would be advisable to other researchers applying this methodology to maintain yeast cells in culture for only few generations following transformation and to induce production of the isoprenoid precursors in galactose-containing media only, immediately prior to analysis.

1.5. Microsomal protein preparation and cytochrome P450 quantification.

Microsomal proteins were prepared from 250 mL yeast cultures as previously described (6) with an additional final ultracentrifugation step at 100,000*g* for 60 min. The quantification of CYPs was performed as described by Omura and Sato (7) , by measuring the binding of CO to the reduced form of CYP enzymes, which occurs with spectroscopic difference at 450 nm, and using the extinction coefficient 91 $mM^{-1}cm^{-1}$. Microsomal preparations from cells carrying CPR2 but an empty vector with respect to CYP genes were used for background correction (negative control).

1.6. GC-MS analysis conditions.

GC-MS analysis was carried on a DB-5 column using helium as a carrier gas with a constant velocity of 40 cm/sec. Different temperature programs were used according to the extraction procedure. Samples resulting from dodecane culture overlays were analyzed using the temperature program described in reference (2), while ethyl acetate or pentane extracted and TMS-derivatized samples were subjected to a temperature program consisting of: initial temperature 60 °C, ramp to 200 °C with a rate of 15 °C/min, hold for 10 min, ramp to 290 °C with a rate of 15 °C/min, hold for 20 min.

1.7. General experimental procedures related to the isolation and structure elucidation of oxidation products.

Optical rotations were measured on a Perkin-Elmer model 341 polarimeter with a 1 dm cell. UV spectra were acquired on a Shimadzu UV-160A spectrophotometer. IR spectra were obtained on a Bruker Tensor 27 spectrometer. NMR spectra were recorded on Bruker AC 200 and Bruker DRX 400 spectrometers. Chemical shifts are given on a δ (ppm) scale using TMS as internal standard. The 2D experiments were performed using standard Bruker pulse sequences. High resolution ESI mass spectrometric data were measured on a Thermo Scientific LTQ Orbitrap Velos mass spectrometer. Low resolution EI mass spectra were measured on either a Hewlett-Packard 5973 mass spectrometer or a Thermo Electron Corporation DSQ mass spectrometer by using a Direct-Exposure Probe. GC-MS analyses were carried out using a Hewlett-Packard 6890 gas chromatograph equipped with a HP-5MS fused silica capillary column (30 m x 0.25 mm; film thickness 0.25 εm), a split-splitless injector and a Hewlett-Packard 5973 MS detector operating in electron ionization mode at 70 eV. Column chromatography separations were performed with Kieselgel 60 (Merck). HPLC separations were conducted using an Agilent 1100 Series liquid chromatography pump equipped with refractive index detector, using an Econosphere Silica 10u (250 mm x 10 mm) or a Chiralcel OD, 10 εm (25 cm x 10 mm) column. TLC were performed with Kieselgel 60 F254 (Merck aluminum support plates) and spots were detected after spraying with 15% H_2SO_4 in MeOH reagent and heating at 100 °C for 1 min.

1.8. Structure elucidation of isolated compounds

Ferruginol (**16**), 11-hydroxy-ferruginol (**17**) and pisiferol (**19**) were isolated in pure form and identified on the basis of their spectroscopic data and comparison with literature values (8-10). The new natural product 11-keto-miltiradiene (**18**) was obtained as a yellow powder. The IR spectrum showed an absorption band at 1674 cm^{-1} indicative for the presence of carbonyl functionalities in the molecule. Its molecular formula was postulated to be $C_{20}H_{30}O$ by a combined analysis of its HRESIMS and ^{13}C NMR data. The ^{13}C NMR spectrum revealed 20 carbon signals, among which four were olefinic and one was a carbonyl. The ^{1}H NMR spectrum of **18** exhibited a high degree of similarity with that of miltiradiene (11). The HSQC, COSY and HMBC spectra of compound **18**

allowed the assignment of the protons and carbons of the molecule. The key heteronuclear correlations of H-12 with C-9, C-11, C-13, C-14 and C-15, of H_2-6 with C-8 and C-10, of H_2-14 with C-8 and C-9, of H-15 with C-13 and of H_3-20 with C-9 indicated the position of the carbonyl group at C-11 (Fig. S14).

1.9. 11-Keto-miltiradiene (18): Yellow powder; $[\alpha]_D^{20}$ +66.0 (*c* 0.5, $CHCl_3$); UV ($CHCl_3$) λ_{max} (log ε) 249 (3.69), 425 (3.25) nm; IR (film) ν_{max} 2931, 2829, 1674; NMR data, see Table S3; HRESIMS *m/z* 285.2231 $[\zeta\ -H]^-$ (calcd for $C_{20}H_{29}O$, 285.2218).

1.10. Isolation of ferruginol-oxidation products

A 1 L culture of AM119 cells expressing the appropriate enzymes in Gal/Raff-SD medium was overlaid with 100 mL of dodecane and incubated in a shake-flask for 2 days. The resulting dodecane layer was distilled in vacuo at 42 °C to afford a concentrated extract (ca. 5 mL) that was submitted to gravity column chromatography using *n*-pentane as the mobile phase in order to remove the remaining volume of dodecane. The column was flushed with EtOAc to retrieve the secondary metabolites. The solvent was evaporated in vacuo to yield an oily residue (0.46 g) which was submitted to gravity column chromatography on silica gel, using cyclohexane with increasing amounts of EtOAc as the mobile phase, to yield 5 fractions (1ï 5). Fraction 2 (115.0 mg) was submitted to normal phase HPLC, using *n*-Hex/ isopropanol (97:3) as eluent, to afford **16** (29.0 mg). Fraction 3 (47.0 mg) was submitted to normal phase HPLC, using *n*-Hex/isopropanol (97:3) as eluent, to afford **16** (25.2 mg) and **18** (4.9 mg). Fraction 4 (57.0 mg) was submitted to normal phase HPLC, using *n*-Hex/ isopropanol (97:3) as eluent, to yield **16** (9.5 mg) and **17** (9.6 mg).

1.11. Isolation of 19.

A 1 L culture of AM119 cells expressing the appropriate enzymes in Gal/Raff-SD medium was overlaid with dodecane as above and incubated in a shake-flask for 2 days. The resulting dodecane phase was distilled and submitted to a gravity column chromatography, as above. The resulting oily residue (0.68 g) was subjected to gravity column chromatography on silica gel, using cyclohexane with increasing amounts of EtOAc as the mobile phase, to yield 7 fractions (1ï 7). Fraction 6 (42.0 mg) was subjected to normal phase HPLC using cyclohexane / acetone (85:15) as eluent and subfraction 6d (7.4 mg) was further purified by normal phase HPLC, using c-Hex/EtOAc (82:18) as eluent, to yield **19** (1.1 mg).

2. Supplementary Tables.

Table S1. The fifteen *S. pomifera* CYPs selected for further characterization from the analysis of Trikka and colleagues listed in order of descending transcript abundance in the cDNA library, according to their corresponding FPKM values produced by the RSEM software (12). Transcript annotation was kindly provided by Prof. David Nelson.

***S. pomifera* transcript**	**Annotation**	**CLAN**	**FPKM**
Unigene29490	CYP76AH24 ortholog	CYP71	2026.30
CL5059.Contig1	CYP76AK6	CYP71	1892.16
Unigene22114	CYP7IBE52	CYP71	1746.15
CL528.Contig2	CYP716A96	CYP85	1326.01
Unigene69	CYP86A92 ortholog	CYP86	868.07
Unigene2012	CYP71D455	CYP71	791.26
Unigene24154	CYP76G16 ortholog	CYP71	204.79
Unigene31529	CYP71AU53 ortholog	CYP71	66.61
CL3375.Contig3	CYP728D17 ortholog	CYP71	55.01
Unigene22595	CYP716C12 ortholog	CYP71	44.40
CL913.Contig1	CYP71CS1	CYP71	15.75
CL2521.Contig1	CYP71A63	CYP71	14.63
CL3408.Contig2	CYP71AU68	CYP72	10.53
CL5645.Contig2	CYP76B64	CYP71	6.07
CL8143.Contig1	CYP76A35 ortholog	CYP86	1.71

Table S2. List of yeast strains used.

Strain	Genotype	Source
AM102	Mat a/Ŭ, P_{GAL1}-*HMG2*(K6R):: HOX2, *ura3, trp1, his3,* P_{TDH3}-*HMG2*(K6R)X2-::*leu2 ERG9/erg9, UBC7/ubc7, SSM4/ssm4*	reference (4)
AM119	Mat a/Ŭ, P_{GAL1}-*HMG2*(K6R)::*HO*x2, *ura3, trp1, his3,* P_{TDH3}-*HMG2*(K6R)X2-::*leu2 ERG9/erg9, UBC7/ubc7, SSM4/ssm4,* P_{TDH3}-*HEM3*::*FLO5*	this study

Table S3. ^{1}H and ^{13}C NMR data (in $CDCl_3$) of **18**.

Position	δ_C[a]	δ_H (*J* in Hz)
1	36.1, CH_2	2.69, m, 0.99, m
2	18.9, CH_2	1.62, m, 1.48, m
3	41.6, CH_2	1.40, m, 1.14, m
4	41.6, C	
5	51.3, CH	1.09, m
6	18.1, CH_2	1.80, dd (13.3, 6.7), 1.50, m
7	33.4, CH_2	2.45, m
8	147.8, C	
9	145.0, C	
10	38.1, C	
11	181.3, C	
12	137.8, CH	6.36, s
13	146.7, C	
14	33.5, CH_2	2.47, m, 2.35, m
15	26.9, CH	2.87, sept (6.8)
16	21.5, CH_3	1.07, d (6.8)
17	21.4, CH_3	1.06, d (6.8)
18	33.8, CH_3	0.90, s
19	21.7, CH_3	0.86, s
20	20.0, CH_3	1.20, s

[a]Chemical shifts of C-9 and C-11 were obtained from their corresponding HMBC correlations.

Table S4. Kinetic parameters of the identified CYPs.

Oxidized carbon	Substrate	Enzyme	k_{cat} (min^{-1})	K_M (μM)
C-11	**16**	CYP76AH24	6.11±0.45	45.84±9.37
	16	CYP76AH4	5.09±0.63	49.63±11.23
	14	CYP76AH24	1.97±0.72	72.63±43.19
	14	CYP76AH4	1.63±0.29	84.04±22.99
C-12	**15**	CYP76AH24	5.51±0.71	20.62±6.12
	15	CYP76AH4	- [a]	25±6[a]
C-2α	**16**	CYP71BE52	0.04±0.002	3.96±0.72
C-20	**16**	CYP76AK6	1.43±0.21	20.81±7.76
	16	CYP76AK8	0.863±0.75	16.24±4.01
	17	CYP76AK6	0.34±0.02	13.18±1.89
	17	CYP76AK8	0.236±0.012	4.84±0.93

[a]Reported by Zi and Peters (13).

Table S5. List of primers.

Gene Name / purpose	Primer	Sequence
HEM3	5-HEM3-EcoRI	gaattcatgggccctgaaactctacatattggtgggagaa
	3-HEM3-XhoI	ctcgagtcatttgattctgtctaaattaatttcatcca
FLO5 locus integration	5-FLO5-COD7	atatcctgcaaacaacacttcgaattcaattcgatatttcataagttacaactaaccagttcgagtttatcattatc
	3-FLO5-COD7	catcctaagcgaaccacactagatcttacgttagtactactgaaaatggcaatggatctgatatcaccta
CDS	SfCDS-BamHI-5	ggatccatggcgcccctgacttgc
	SfCDS-3xGS-MfeI	caattggctaccgctgccgctacctacgaccggtccaaagagtactt
CYP76AH4	RoFS-EcoRI	gaattcaaaaaaatggctaagaaaacctcgtcc
	RoFS-NotI	gcggccgcttagcttttaacaatcgggataa
pESC-Leu vector mutagenesis	pESC-noEcoRI	gaaccttcaatgtagggaactcgttcttgatggtttcctcc
CPR2 gene mutagenesis	CPR2-noEcoRI	gttgagcacactcctttgtggattcgacctgctggtg
CYP76AH24	5-U29490-EcoRI	gaattcatgtctgatcccttccctcttgtagctg
	3-U29490-NotI	gcggccgctcacgccttaatcggaacga
CYP76AK6	5-CL5059-EcoRI	gaattcatgcaagttctcatccttctttctctggccttcctagca
	3-CL5059-NotI	gcggccgctcaaactttgatgggaatagctcttaggggggattttcttct
CYP71BE52	5-U22114-EcoRI	gaattcatggagacagagtccaatcatcttctctggaagttcac
	3-U22114-NotI	gcggccgcttatttggtgggcaaagttcttttgattgccggaataag
CYP716A96	5-CL528-MfeI	caattgatggaggtcttgtacgtctcactcctctcgggctt
	3-CL528-NotI	gcggccgctcaagccttgtgagggtaaagacgaacaggcaatccc
CYP86A92 ortholog	5-U69-1-MfeI	caattgatgggggggggcttatggtatgt
	3-U69-1-NotI	gcggccgctcaattttcgcttttcccaattttg
CYP71D455	5-U2012-EcoRI	gaattcatggagacagagtccaatcatcttctctggaagttcac
	3-U2012-NotI	gcggccgctcacaagggtggttcataaggagtagcaacaacaaaaag
CYP76G16 ortholog	5-U24154-EcoRI	gaattcatggactatgagattgcgggcattgtcatagccctactaa
	3-U24154-NotI	gcggccgctcatttccacacatatggaatgggtatagccctcaacgg
CYP71AU53 ortholog	5-U31529-MfeI	caattgatgaatattatcaaagctttttttcaagaacaatatcaaag
	3-U31529-NotI	gcggccgctcatgtagccttagaggcaactgcaactagaggaatag
	5-U31529-noMfeI	aaagacgaagagatgcaactggatttcattcatttttgtg
CYP728D17 ortholog	5-CL3375-EcoRI	gaattcatggagtcaaccattttgttgtcactcctcgcctttctc
	3-CL3375-NotI	gcggccgcttattcatctaaaggcttcttcatcttgatctgt
CYP716C12 ortholog	5-U22595-EcoRI	gaattcatggagctcctaacagtggctatctccatactcc
	3-U22595-NotI	gcggccgctcaatgttggtaaagccggacgggcaaacctttcttggg
	5-U22595-noEcoRI	ttgccgaagaggaactcgacgctctcgccca
CYP71CS1	5-CL913-MfeI	caattgtggaggatttccacttttacacacttcctctcactcttc
	3-CL913-NotI	gcggccgcctaaacgtcggaattgatagttgcaacaacaatgagtg
CYP71A63	5-CL2521-EcoRI	gaattcatggttgctctactacttctttttctcttccattttcc
	3-CL2521-NotI	gcggccgcttaaactacttcagaggcacgagaagtagcaaccac
CYP71AU68	5-CL3408-MfeI	caattgatggatgctcaagaaatatgtattcaagcatcaaa
	3-CL3408-NotI	gcggccgcttacatccaaatcctcacattttgctccattagcc
CYP76B64	5-CL5645-EcoRI	gaattcatggatttccttacaatctccgtt
	3-CL5645-NotI	gcggccgctcaagttcaatccccaacgctt
CYP76A35 ortholog	5-CL8143-MfeI	caattgatgctcaaaactaactcaaaaatggcgtggcttgtttcac
	3-CL8143-NotI	gcggccgcttagactcctctttctcttggaactgctttcagaggtgtca

3. Supplementary Figures

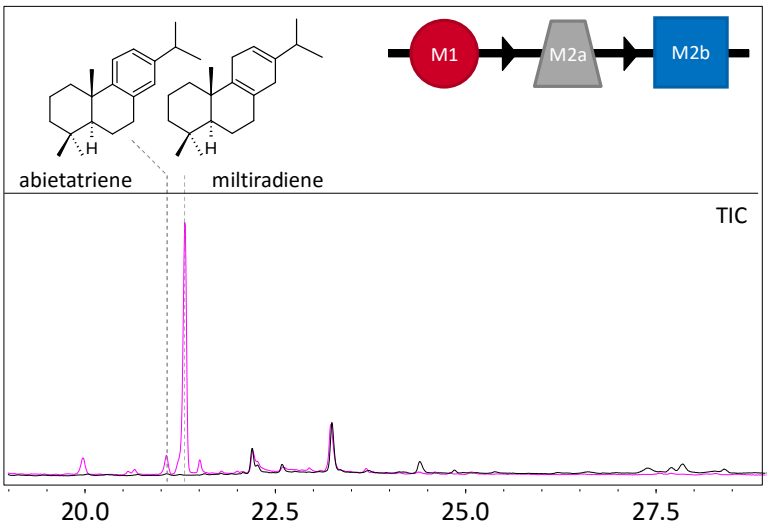

Figure S1. Production of 14 in yeast cells. Co-expression of the class II enzyme, SfCDS, responsible for synthesis of **13** from **12**, with the class I miltiradiene synthase, SpMilS, resulted in the production of **14** in yeast cells. **14** converts spontaneously to **15** *in vitro* or in yeast cells. TIC GC-MS chromatogram is presented alongside a diagrammatic description of the modular design.

A

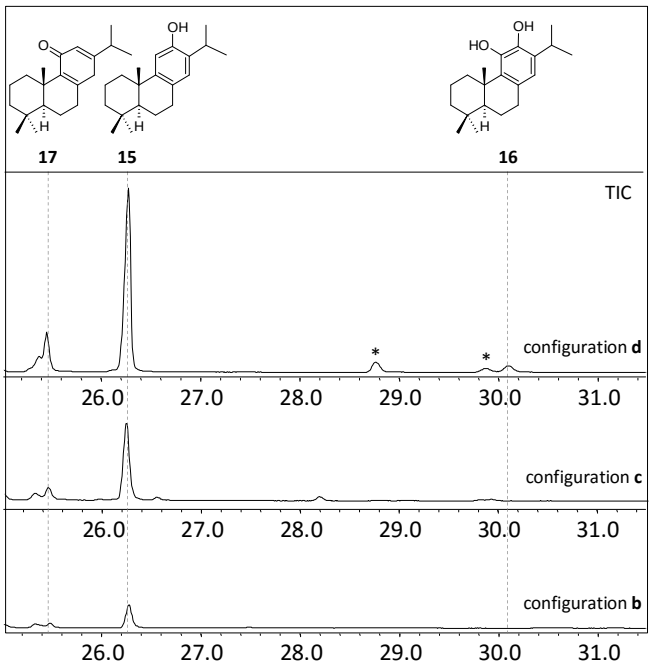

B

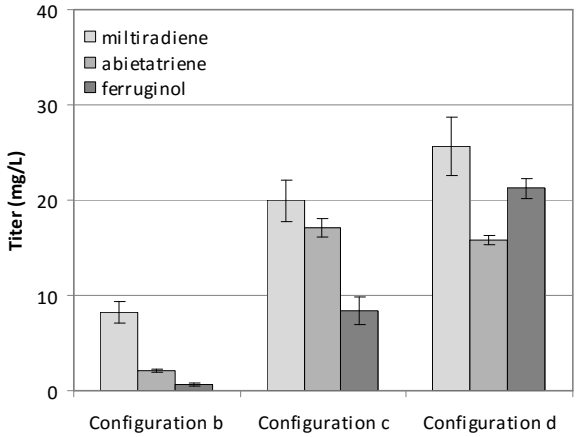

Figure S2. Determination of oxidation efficiency in the optimized yeast strains. A. Expression of the CYP76AH24 ortholog in miltiradiene-producing yeast cells, in the initial configuration (Fig. 2A, panel **b**), resulted in the production of **16**. With the gradual improvement of the yeast platform (configurations **c** and **d**, Fig. 2A, panels **c** and **d**), the formation of **17** and **18** became apparent. The two peaks indicated by asterisks correspond to degradation products of **17**. **B.** In the basic platform configuration (configuration **b** in Figure 3) 32% of **15** (gray), resulting from the spontaneous oxidation of **14** (light gray), was converted to **16** (dark gray). A similar conversion efficiency was achieved in the modified platform carrying a fusion of the M1 and M2a-specific parts (configuration **c** in Figure 3), despite a 3-fold increase in the titer of all three compounds. The platform expressing the *HEM3* gene from a single copy chromosomal integration (configuration **d** in Figure 3) achieved 62% conversion of **15** to **16**, reaching a titer of 21.2 mg/L.

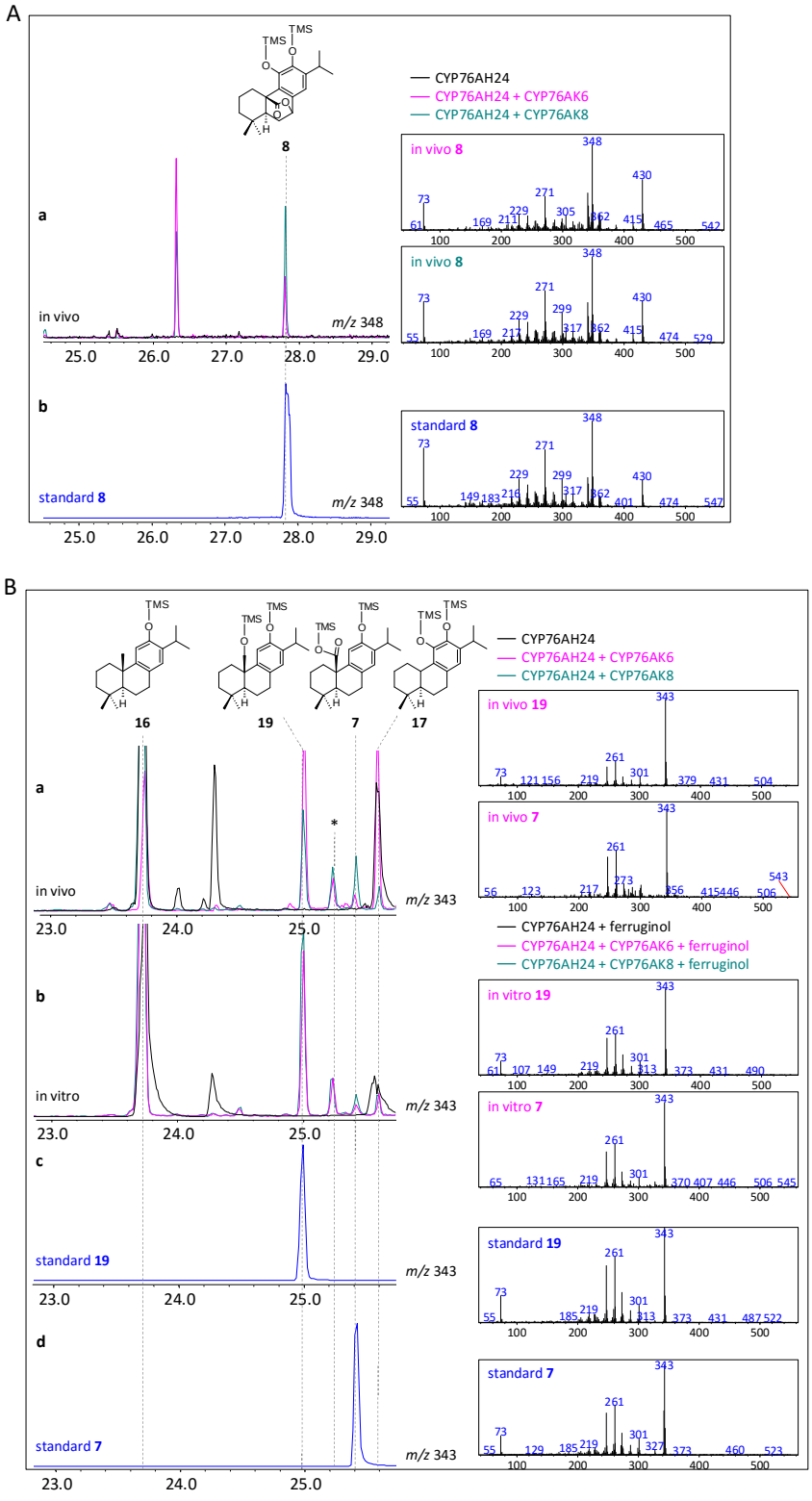

Figure S3. CYP76AK6 (pink) and its homolog, CYP76AK8 (teal), catalyze successive oxidation events at C-20. A. Identification of **8** in carnosic acid-producing yeast cells by GC-MS (panel **a**) and comparison with reference standard (blue) (panel **b**). **B.** Formation of **19** and **7** by CYP76AK6 and CYP76AK8 in yeast cells co-expressing CYP76AH24 and SpMilS (panel **a**) or *in vitro* by microsomal preparations of the two CYPs using **16**

as substrate (panel **b**). Chromatograms and mass spectra of authentic standards of **19** and **7** (blue) are shown in panel **c** and panel **d**, respectively.

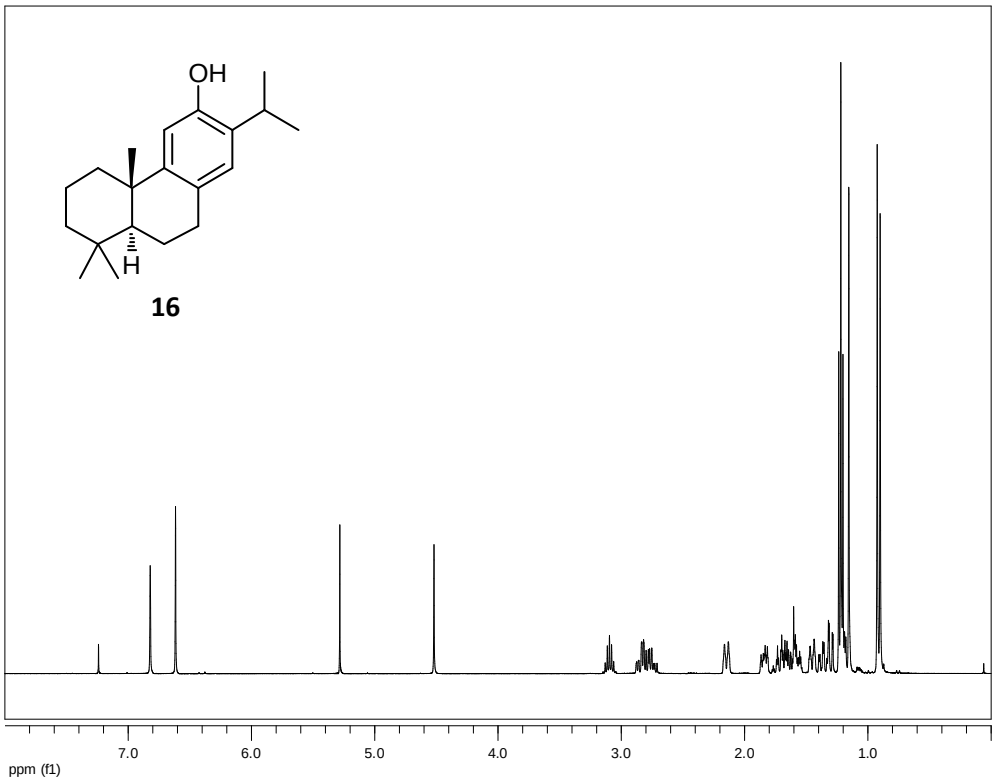

Figure S4. ^{1}H NMR spectrum of **16**.

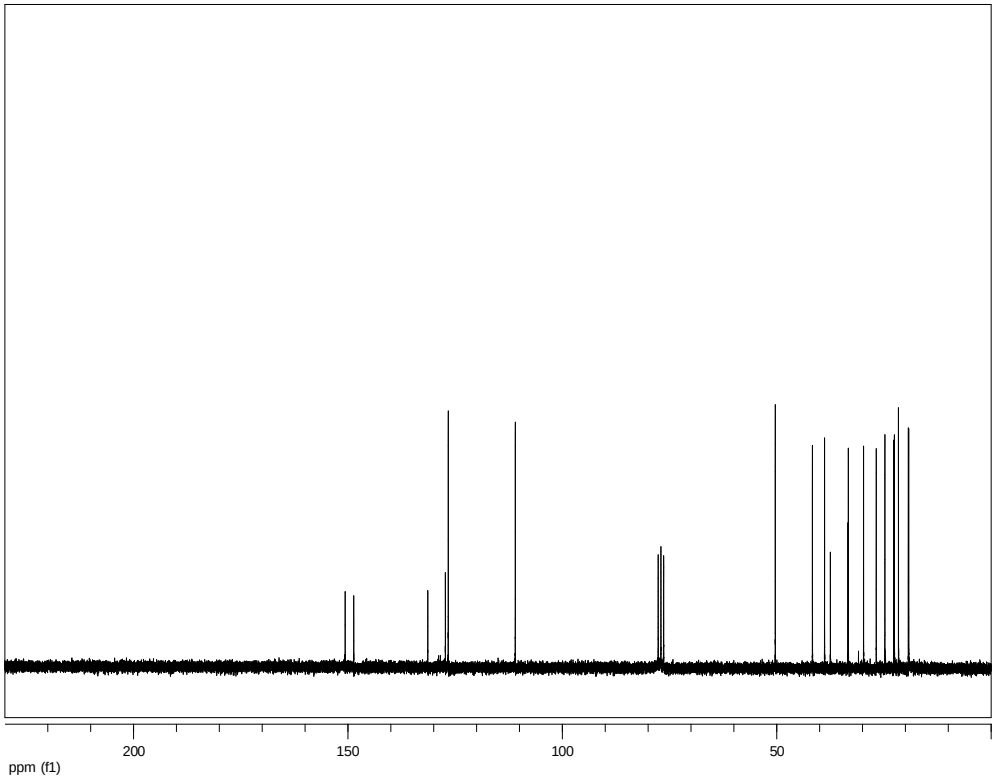

Figure S5. ^{13}C NMR spectrum of **16**.

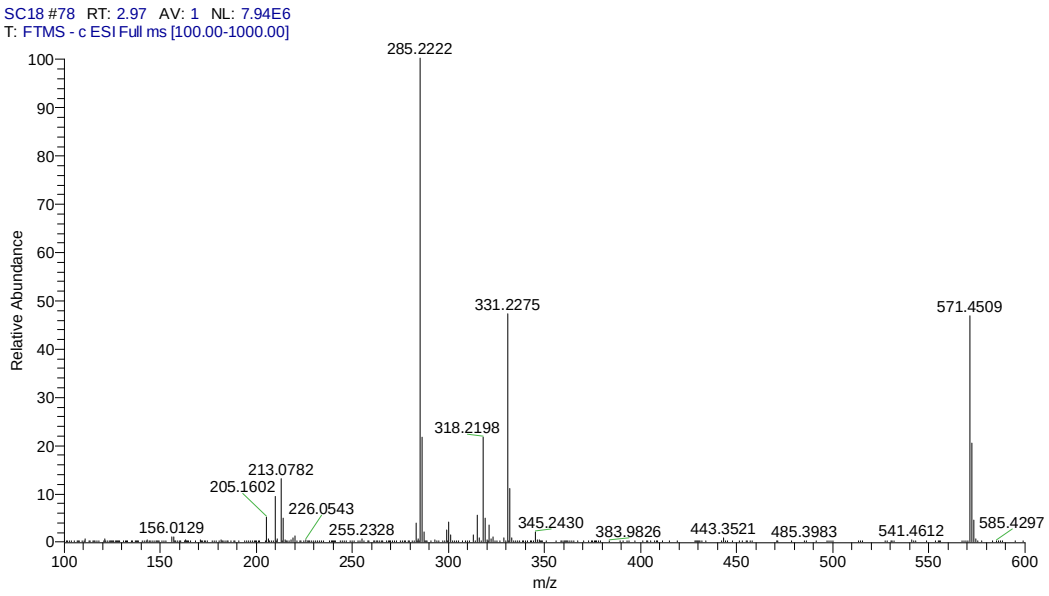

Figure S6. HR-ESI-MS spectrum of **16**.

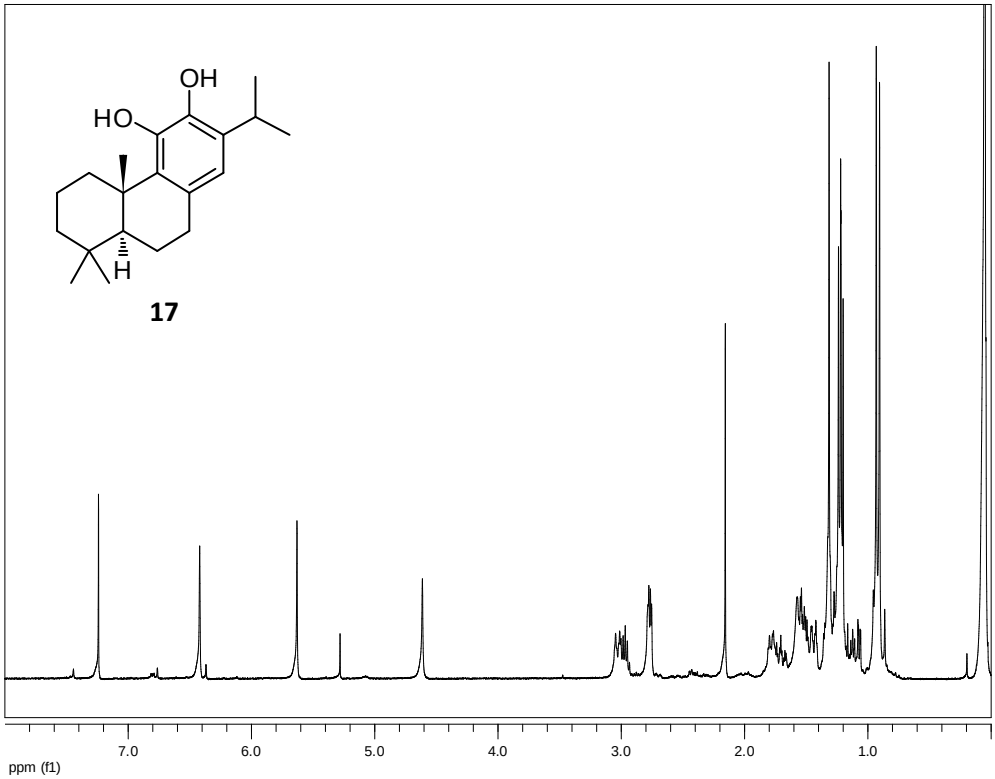

Figure S7. ^{1}H NMR spectrum of **17**.

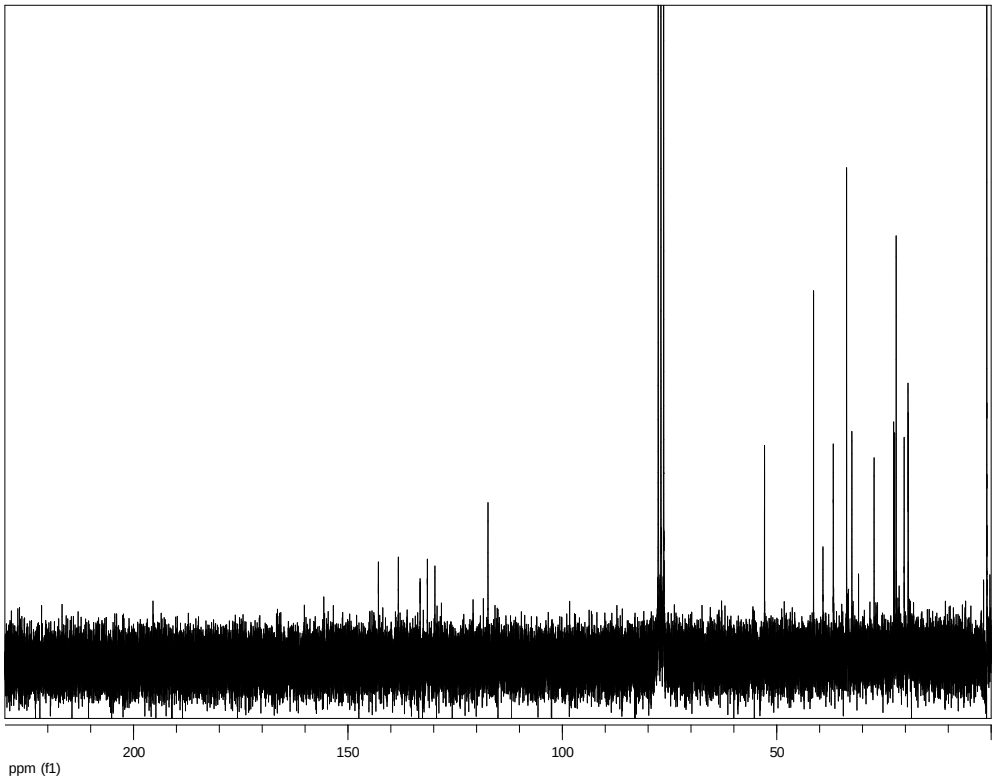

Figure S8. ^{13}C NMR spectrum of **17**.

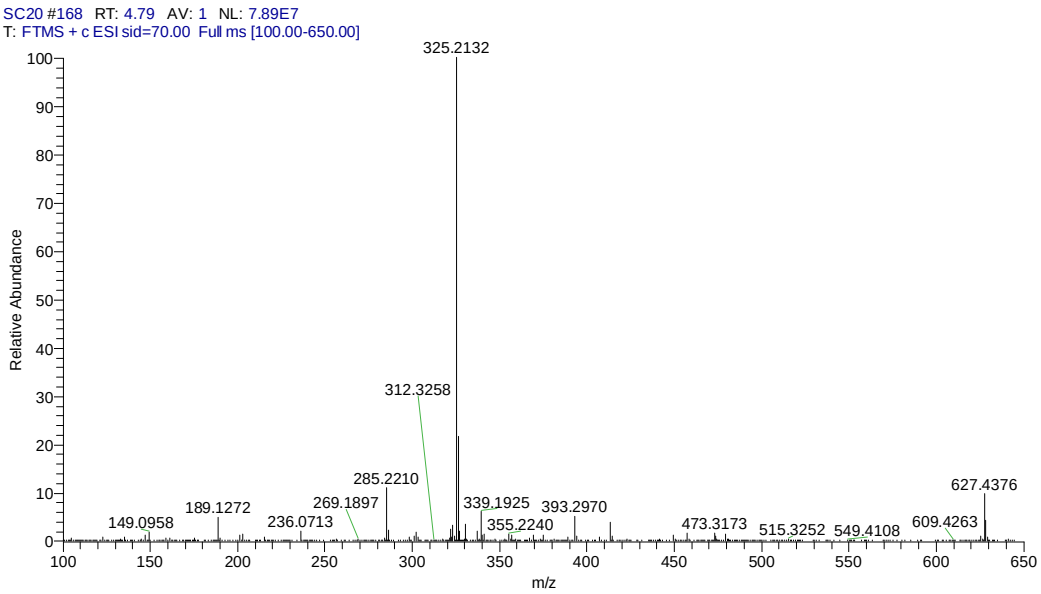

Figure S9. HR-ESI-MS spectrum of **17**.

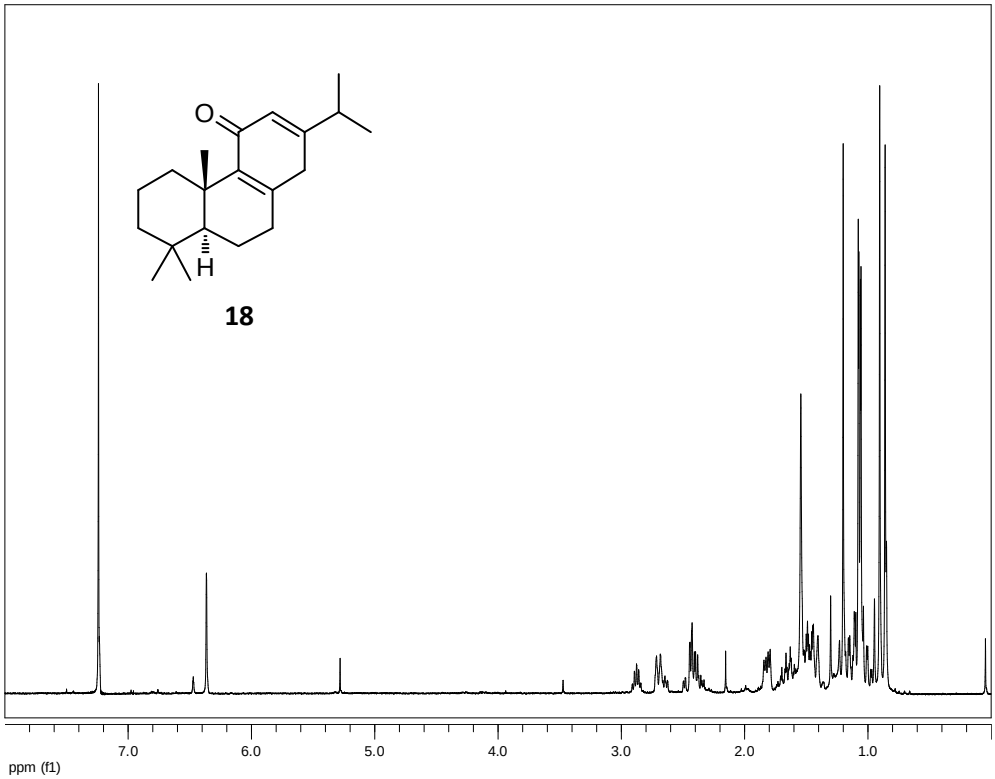

Figure S10. ^{1}H NMR spectrum of **18**.

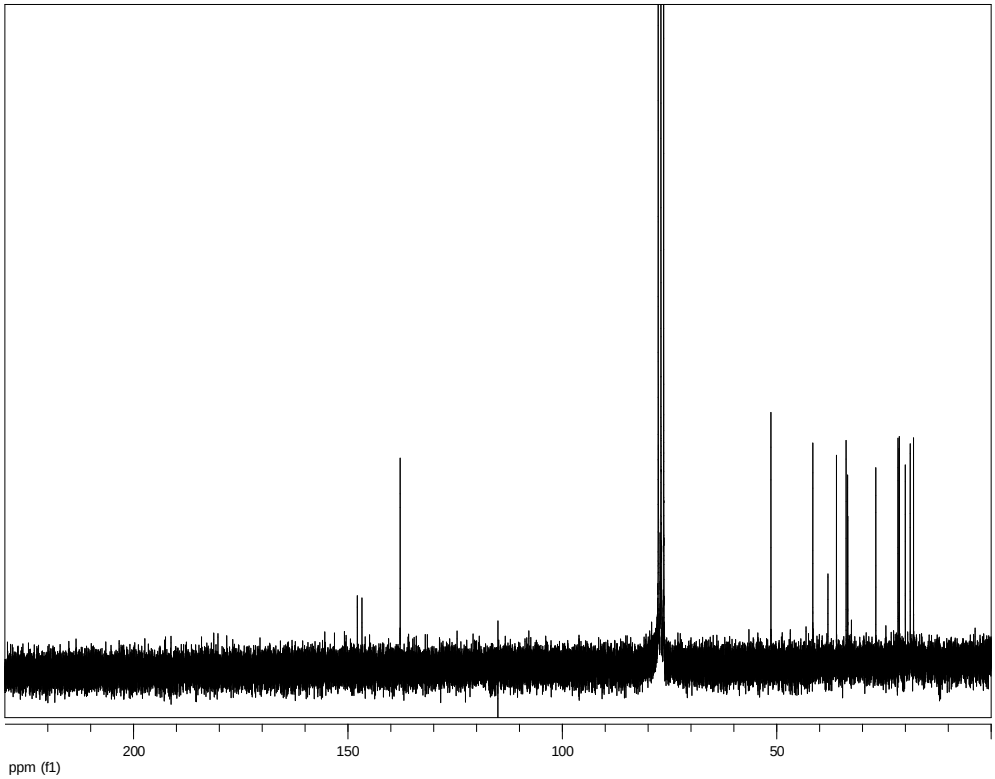

Figure S11. ^{13}C NMR spectrum of **18**.

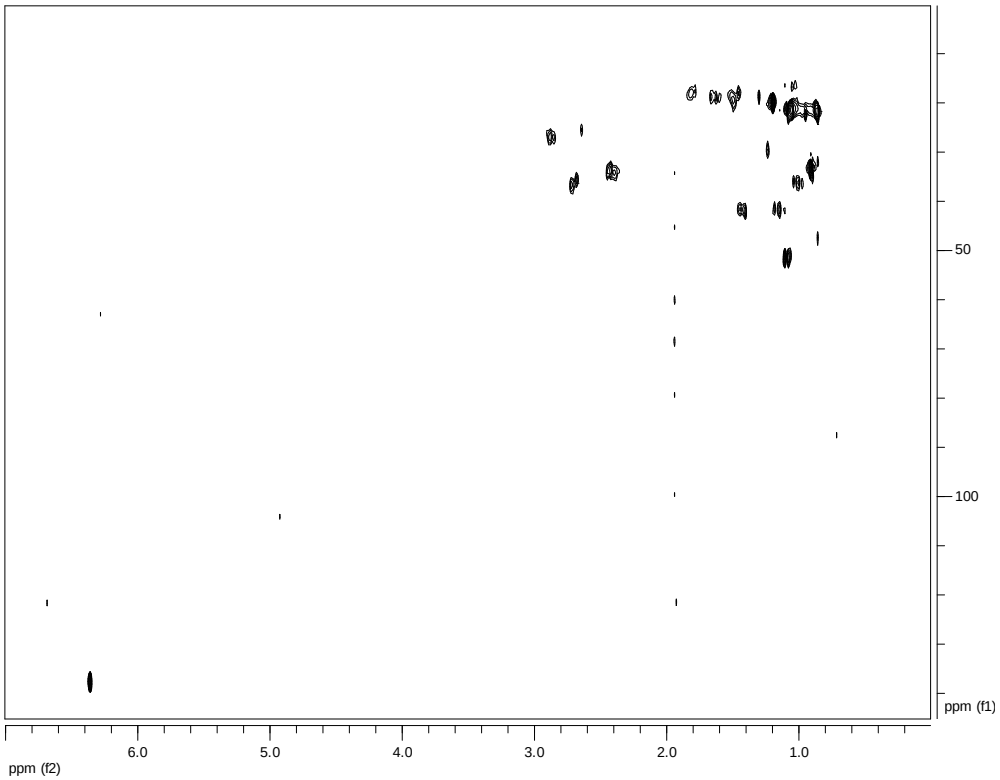

Figure S12. HSQC-DEPT spectrum of **18**.

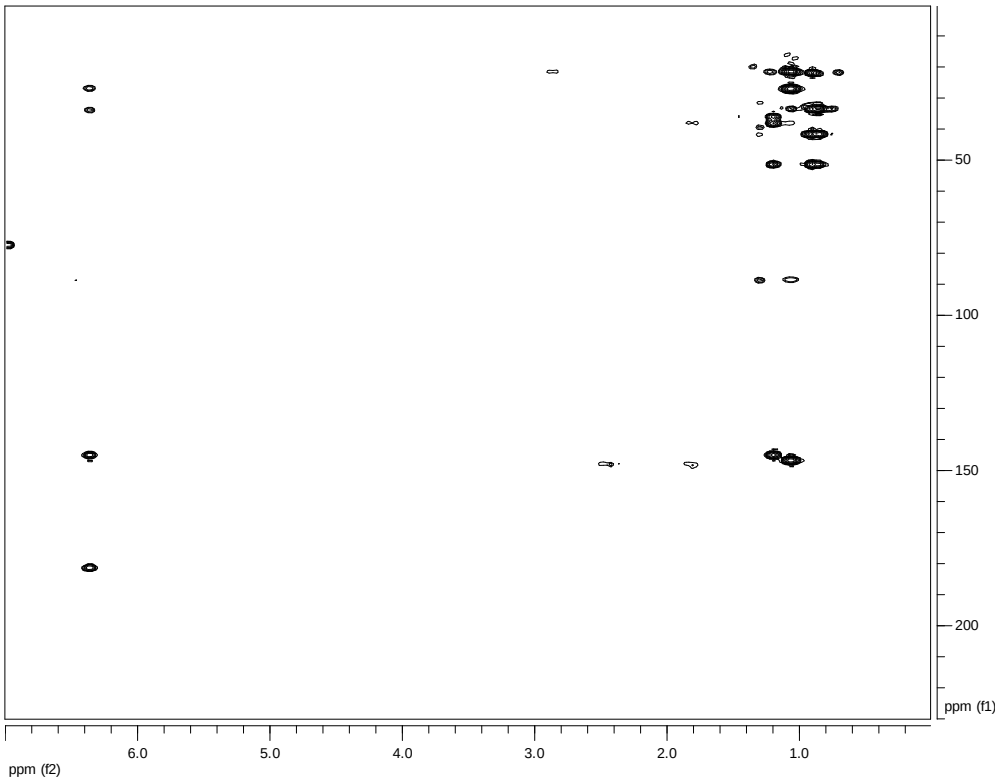

Figure S13. HMBC spectrum of **18**.

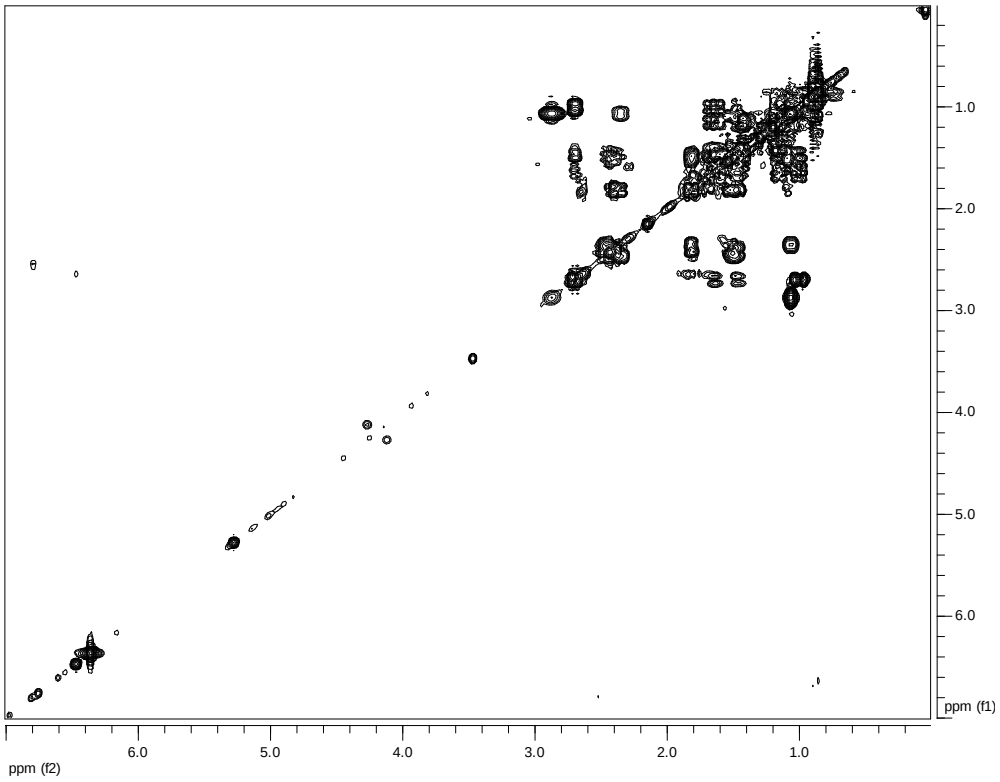

Figure S14. COSY spectrum of **18**.

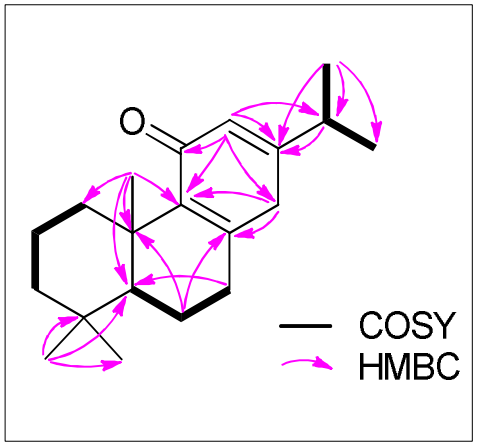

Figure S15. COSY (bold lines) and important HMBC (arrows) correlations observed for **18**.

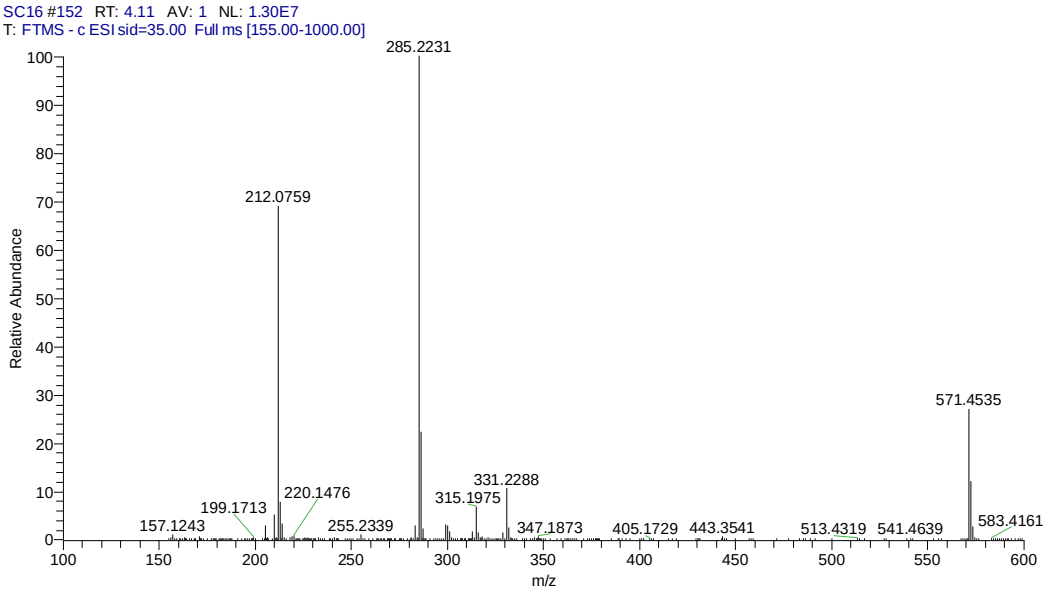

Figure S16. HR-ESI-MS spectrum of **18**.

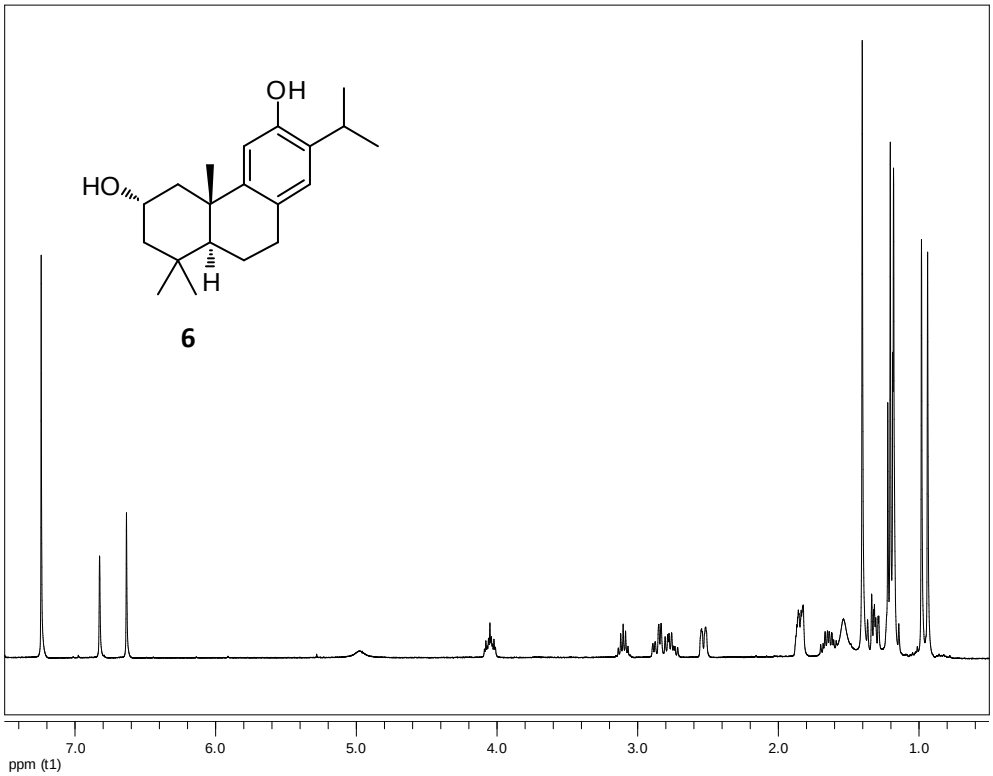

Figure S17. ^{1}H NMR spectrum of **6**.

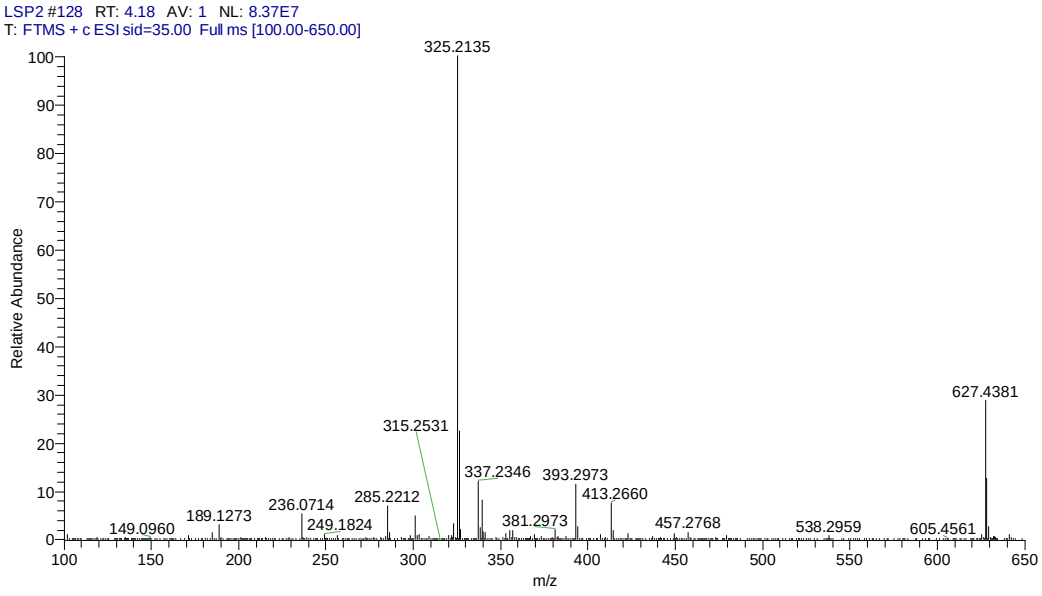

Figure S18. HR-ESI-MS spectrum of **6**.

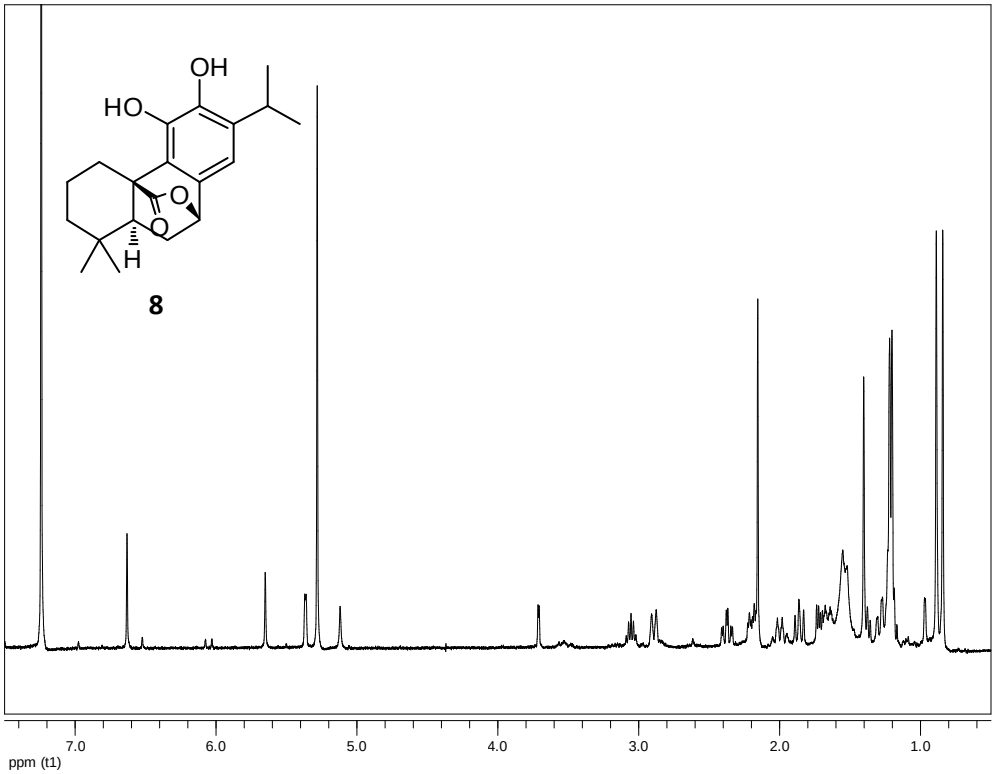

Figure S19. ^{1}H NMR spectrum of **8**.

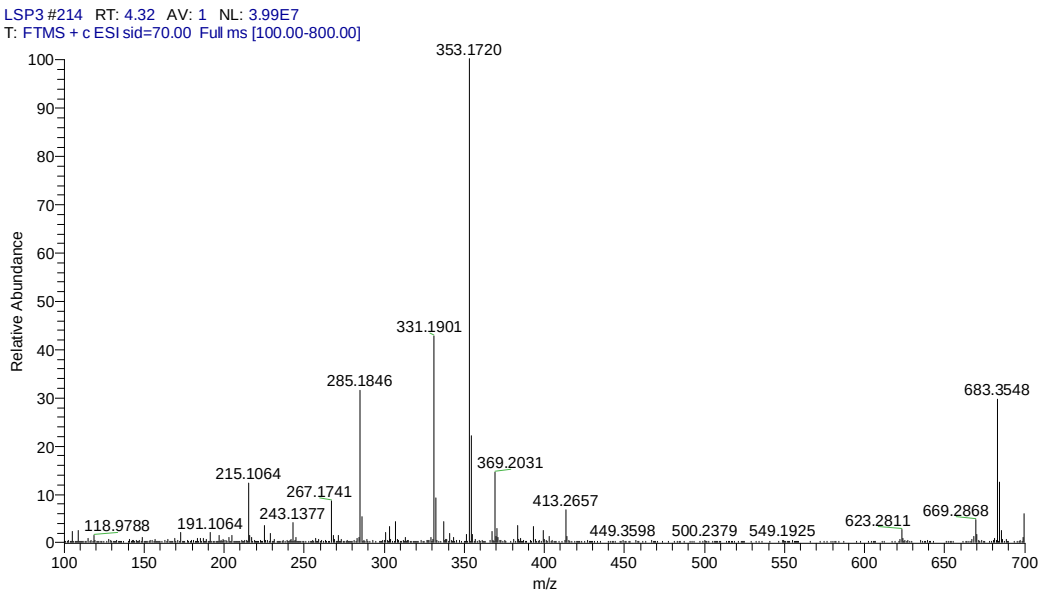

Figure S20. HR-ESI-MS spectrum of **8**.

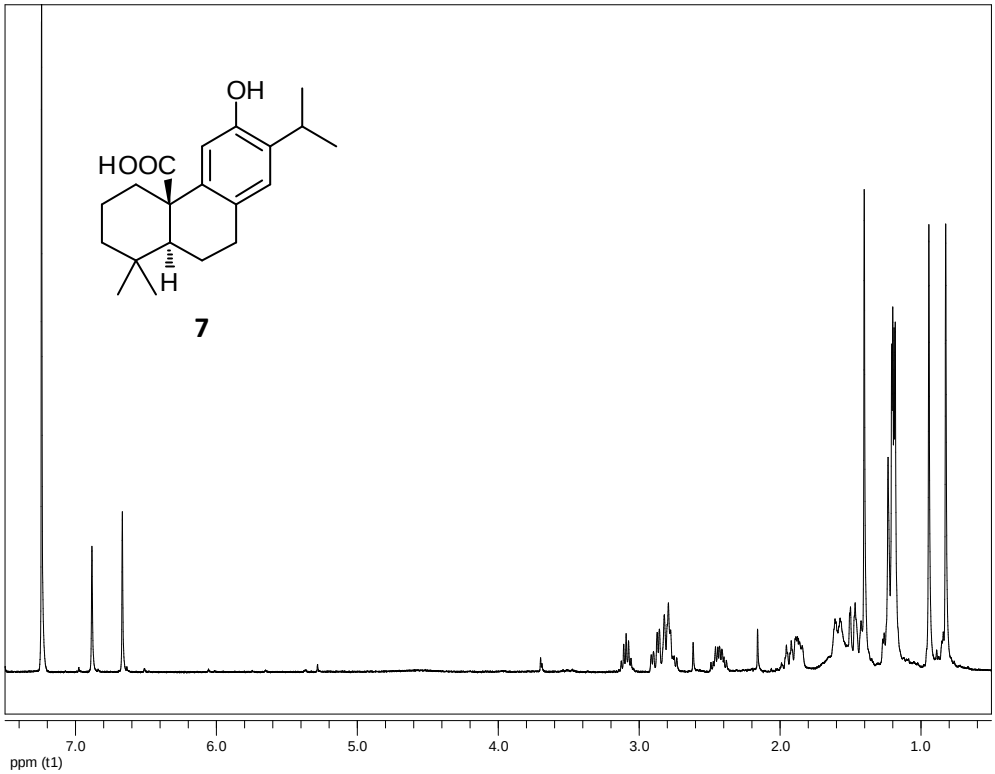

Figure S21. ^{1}H NMR spectrum of **7**.

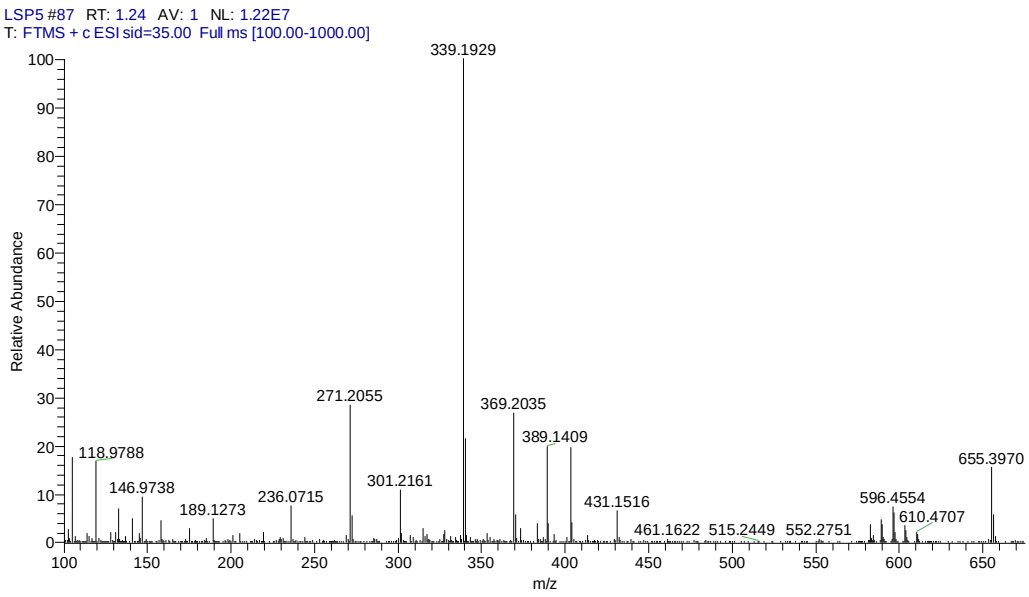

Figure S22. HR-ESI-MS spectrum of **7**.

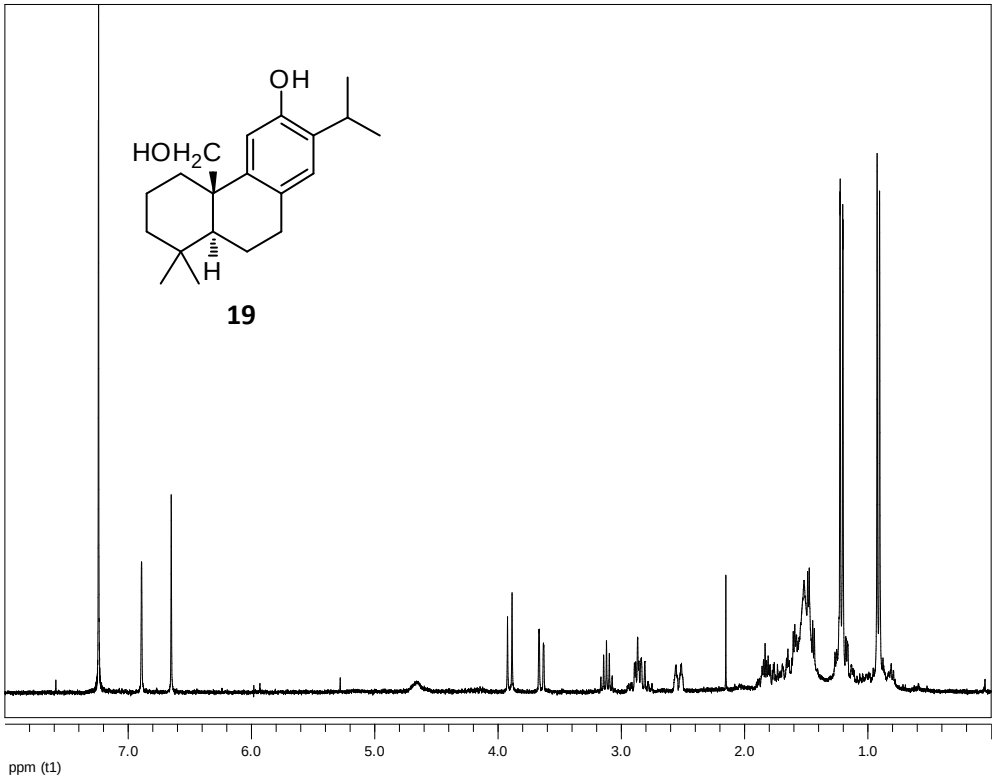

Figure S23. ^{1}H NMR spectrum of **19**.

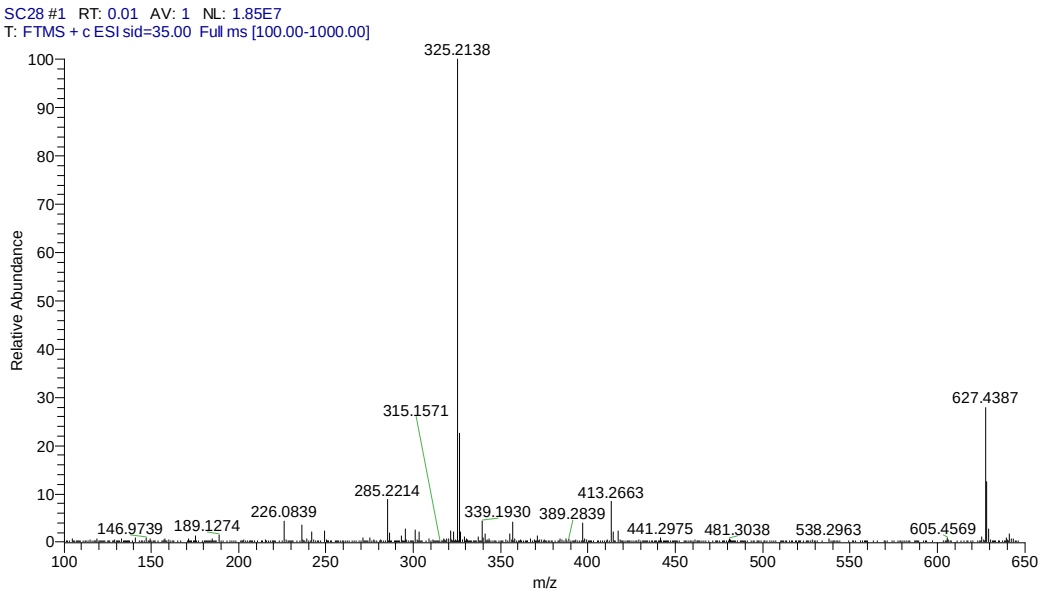

Figure S24. HR-ESI-MS spectrum of **19**.

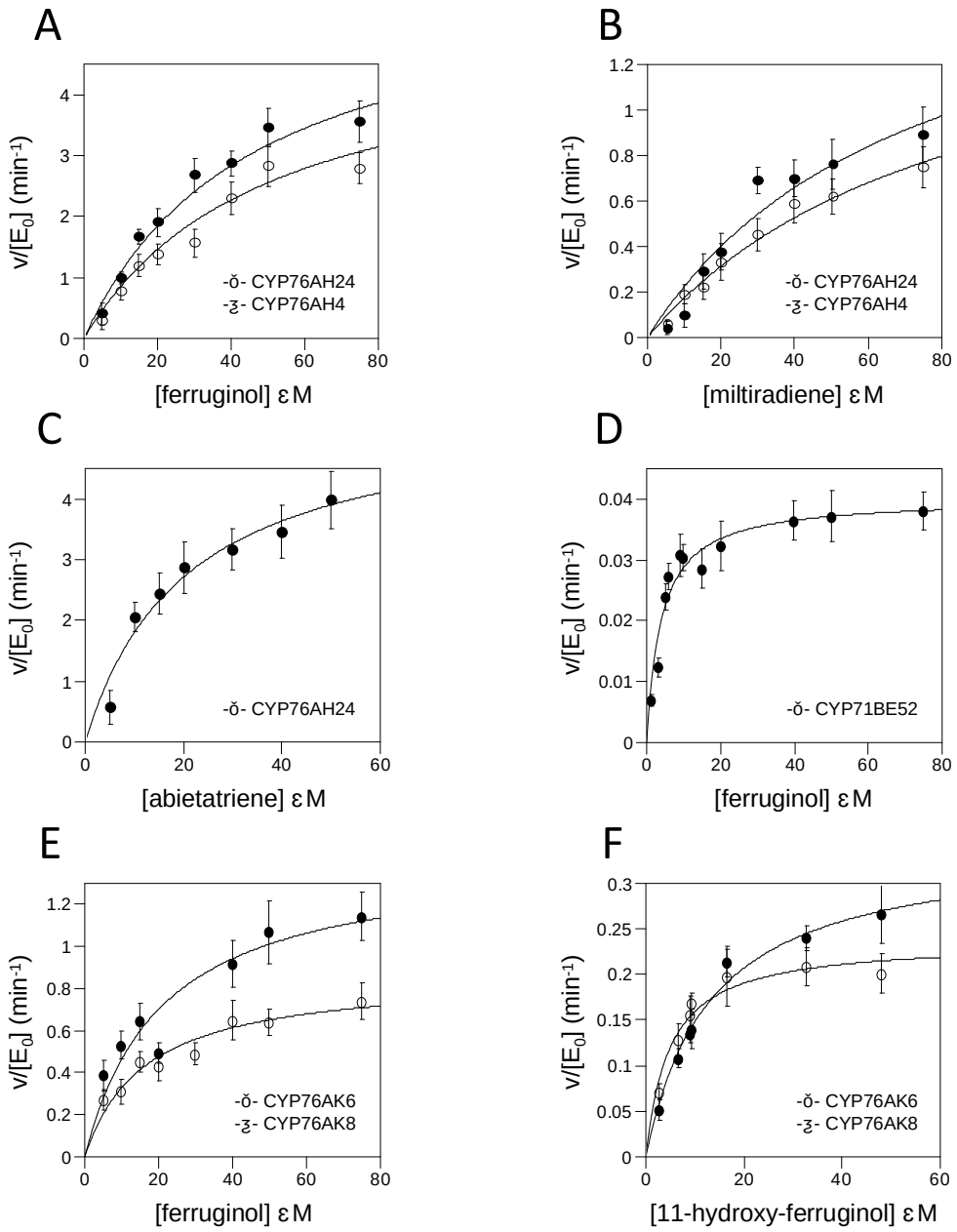

Figure S25. Steady-state kinetic analysis of the oxidation of various labdane-type diterpenes by the *S. pomifera* and *R. oficinalis* CYPs. A. Oxidation of **16** by CYP76AH24 and CYP76AH4. **B.** Oxidation of **14** by CYP76AH24 and CYP76AH4. **C.** Oxidation of **15** by CYP76AH24. **D.** Oxidation of **16** by CYP71BE52. **E.** Oxidation of **16** by CYP76AK6 and CYP76AK8. **F.** Oxidation of **17** by CYP76AK6 and CYP76AK8. Reaction conditions described in the Materials and Methods section.

REFERENCES

1. Ignea C*, et al.* (2015) Reconstructing the chemical diversity of labdane-type diterpene biosynthesis in yeast. *Metab Eng* 28:91-103.
2. Ignea C*, et al.* (2015) Efficient diterpene production in yeast by engineering Erg20p into a geranylgeranyl diphosphate synthase. *Metab Eng* 27:65-75.
3. Ro DK, Ehlting J, & Douglas CJ (2002) Cloning, functional expression, and subcellular localization of multiple NADPH-cytochrome P450 reductases from hybrid poplar. *Plant Physiol* 130(4):1837-1851.
4. Ignea C*, et al.* (2012) Positive genetic interactors of HMG2 identify a new set of genetic perturbations for improving sesquiterpene production in Saccharomyces cerevisiae. *Microb Cell Fact* 11(1):162.
5. Kampranis SC*, et al.* (2007) Rational conversion of substrate and product specificity in a salvia monoterpene synthase: structural insights into the evolution of terpene synthase function. *Plant Cell* 19(6):1994-2005.
6. Pompon D, Louerat B, Bronine A, & Urban P (1996) Yeast expression of animal and plant P450s in optimized redox environments. *Methods Enzymol* 272:51-64.
7. Omura T & Sato R (1962) A new cytochrome in liver microsomes. *J Biol Chem* 237:1375-1376.
8. Dellar JE, Cole MD, & Waterman PG (1996) Antimicrobial abietane diterpenoids from Plectranthus elegans. *Phytochemistry* 41(3):735-738.
9. Kagawa K*, et al.* (1993) Platelet aggregation inhibitors in a Bhutanese medicinal plant, shug chher. *Chem Pharm Bull (Tokyo)* 41(9):1604-1607.
10. Tada M, Kurabe J, Yoshida T, Ohkanda T, & Matsumoto Y (2010) Syntheses and antibacterial activities of diterpene catechol derivatives with abietane, totarane and podocarpane skeletons against methicillin-resistant Staphylococcus aureus and Propionibacterium acnes. *Chem Pharm Bull (Tokyo)*58(6):818-824.
11. Dai Z, Liu Y, Huang L, & Zhang X (2012) Production of miltiradiene by metabolically engineered Saccharomyces cerevisiae. *Biotechnol Bioeng* 109(11):2845-2853.
12. Trikka FA*, et al.* (2015) Combined metabolome and transcriptome profiling provides new insights into diterpene biosynthesis in S. pomifera glandular trichomes. *BMC Genomics* 16(1):935.
13. Zi J & Peters RJ (2013) Characterization of CYP76AH4 clarifies phenolic diterpenoid biosynthesis in the Lamiaceae. *Org Biomol Chem* 11(44):7650-7652.